

# Estimation of Turbulent Mixing From Towed Observations in Narragansett Bay

Dave Ullman, Dave Hebert, and Chris Piecuch  
 Graduate School of Oceanography  
 University of Rhode Island  
 d.ullman@gso.uri.edu

## I. Introduction

The upper reaches of Narragansett Bay have experienced episodic hypoxia during recent years. These events typically impact sub-pycnocline waters of the shipping channel in the Providence River as well as shallower areas such as Greenwich Bay (Figure 1). Hypoxic conditions generally develop during neap tide conditions following surface phytoplankton blooms (Bergondo et al., 2004), but the fact that hypoxia is not observed during all neap tide periods suggests an interplay with other forcing functions including freshwater runoff, nutrient input, and surface fluxes of heat and momentum.

As part of an interdisciplinary investigation of the hypoxia phenomenon in Upper Narragansett Bay, we have recently begun a study of the spatial and temporal variability of turbulent mixing in the Upper Bay. The observations reported here were obtained during summer 2004 during two neap tide periods (July 13-15 and August 10-12) and one spring tide period (July 28-30). During each day of each 3-day period, an approximately 20 km transect (Figure 1) was surveyed using an Acrobat towed undulating vehicle and a vessel-mounted 600 kHz ADCP. The Acrobat, shown in Figure 2, carried a sampling package (Towed Oceanographic Microstructure and Auxiliary Sensors Instrument (TOMASI) built by RGL Consulting Ltd.) that included sensors for temperature, conductivity, and velocity shear microstructure, as well as CTD, oxygen, chlorophyll fluorescence, and dissolved nitrate sensors.

## II. Mixing Estimation from Towed Microstructure Observations.

Assuming homogeneous, stationary, and isotropic turbulence, the temperature variance dissipation rate ( $\chi_T^2$ ) is defined in terms of the temperature gradient measured along the path ( $\epsilon$ ) of an instrument:

$$\chi_T^2 = 6D_T \left\langle \left( \frac{\partial T}{\partial s} \right)^2 \right\rangle = 6D_T \int_0^\infty S_T^2(k) dk$$

where  $S_T(k)$  is the temperature gradient spectrum and  $D_T$  is the molecular diffusivity for heat. The vertical eddy diffusivity ( $K_T$ ) is related to  $\chi_T^2$  by:

$$K_T = \frac{\chi_T^2}{\left\langle \left( \frac{\partial T}{\partial z} \right)^2 \right\rangle}$$

Measurement of  $\chi_T^2$  requires resolution of temperature structures at scales of the order of the Batchelor wavenumber,  $k_{BP} = (\epsilon/\nu D_T^2)^{1/4} / 2\pi$  where  $\epsilon$  is the dissipation rate of turbulent kinetic energy and  $\nu$  is the molecular viscosity. For typical dissipation rates  $k_{BP} \approx 0(100)$  cycles per meter (cpm), and with thermistors, which have relatively slow response times, resolution of these scales is only achievable at very low instrument speeds ( $0(0.1)$  m/s). Conductivity sensors, which are spatially limited but do not exhibit the temporal response of thermistors, can resolve these scales at higher tow speeds.

Because conductivity in seawater is a function of both temperature and salinity, estimation of  $\chi_T^2$  from microconductivity measurements requires that the effects of salinity fluctuations on conductivity be accounted for. Linearizing about a reference state ( $C_0, T_0, S_0$ ), conductivity fluctuations can be approximated by:

$$C' = C_0(AT' + BS')$$

where:  $A = \frac{1}{C_0} \left( \frac{\partial C}{\partial T} \right)$  and  $B = \frac{1}{C_0} \left( \frac{\partial C}{\partial S} \right)$ .

Washburn et al. (1996) show that the conductivity gradient spectrum can be written as the sum of components due to temperature, salinity, and their cross-spectrum:

$$S_c(k) = C_0^2 \left[ A^2 S_T(k) + B^2 S_S(k) + 2AB \frac{m}{|m|} [S_T(k)S_S(k)]^X \right]$$

The cross-spectral contribution (third term on right) depends on the sign of the slope of the local T-S relationship  $m = \langle dS/dT \rangle$  and whether it is assumed that T-S fluctuations are correlated at high wavenumbers. The third term on the right is zero if T-S fluctuations are not correlated. Examples of conductivity gradient spectra illustrating the spectral dependence on  $m$  are shown in Figure 3.

Washburn et al. (1996) further present a method for correcting  $\chi_T^2$  estimates derived from conductivity measurements for the effects of both salinity and a known, finite sensor response ( $H(k)$ ). If  $\chi_T^c$  represents the estimate of  $\chi_T^2$  based on integration of the measured conductivity spectrum ( $S_c(k)$ ):

$$\chi_T^c = \frac{6D_T}{C_0^2 A^2} \int_0^\infty S_{c,c}(k) dk = \frac{6D_T}{C_0^2 A^2} \int_0^\infty |H^2(k)| S_c(k) dk$$

then a correction factor, giving the ratio of measured ( $\chi_T^c$ ) to true dissipation rate can be defined:

$$E = \frac{\chi_T^c}{\chi_T} = f(\epsilon, H(k), m)$$

With assumption of specific spectral forms (Batchelor is used here), the correction factor can be evaluated if the sensor response and the T-S slope are known and if an assumption of the high wavenumber T-S correlation is made. Note that because the magnitude of the Batchelor spectra of T and S are proportional to  $\epsilon$ , the correction factor is independent of  $\chi_T^2$  and depends only on the kinetic energy dissipation rate, the sensor response, and the local T-S slope.

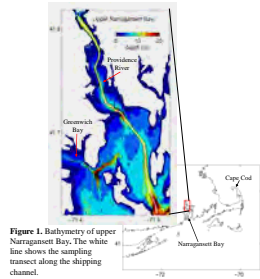


Figure 1. Bathymetry of upper Narragansett Bay. The white line shows the sampling transect along the shipping channel.



Figure 2. Towed Undulating Vehicle (Acrobat) with Microstructure Instrument (TOMASI).

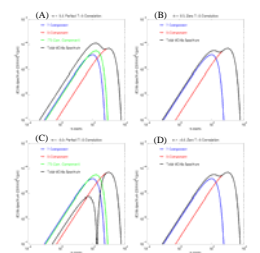


Figure 3. Examples of theoretical conductivity spectra for different values of the T-S slope ( $m$ ) and the degree of correlation of T and S at high wavenumbers. An ideal sensor is assumed. (A) and (B) show the case of  $m=0$  and (C) and (D) show the  $m < 0$  case. The measured conductivity gradient variance exceeds the variance due to temperature alone in all cases except (C). In (C), the effect of salinity fluctuations is a reduction in conductivity variance.

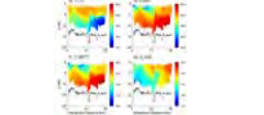


Figure 4. Vertical sections of (a) temperature, (b) salinity, (c)  $\sigma$ , and (d) oxygen concentration during ebb tide on 7/14/2004 along the transect shown in Figure 1.

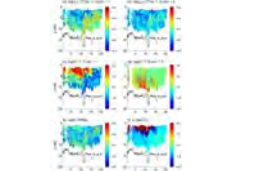


Figure 5. Vertical sections of corrected  $\chi_T^2$  and the correction factor assuming perfect T-S correlation in (a, c) and zero T-S correlation in (b, d) during ebb tide on 7/14/2004 along the transect shown in Figure 1. The estimates of  $\epsilon$  and  $m$  used in computation of the correction factor are shown in (e) and (f).

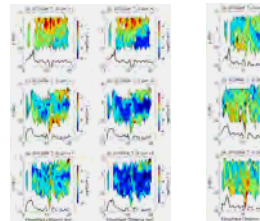


Figure 6. Estimated thermal eddy diffusivity versus depth and distance from north end of transect for July 13-15, 2004. The correction factor for  $\chi_T^2$  was computed assuming perfect T-S correlation in (a), (c), (e), and zero T-S correlation in (b), (d), (f).

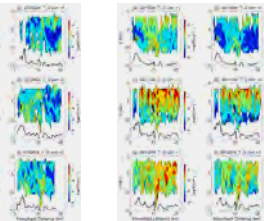


Figure 7. Estimated thermal eddy diffusivity versus depth and distance from north end of transect for July 28-30, 2004. The correction factor for  $\chi_T^2$  was computed assuming perfect T-S correlation in (a), (c), (e), and zero T-S correlation in (b), (d), (f).

## III. Measurements and Analysis

Microstructure conductivity measurements were made using TOMASI's Sea-Bird SBE-7 microconductivity sensor. Macro-scale temperature and conductivity were measured with standard Sea-Bird sensors (SBE-3, SBE-4) sampled at 32 Hz. These conductivity measurements were used to calibrate the microconductivity sensor. The conductivity gradient signal was filtered using an elliptic low pass filter with a cutoff frequency of 300 Hz and then digitized at 1024 Hz. The frozen field approximation was invoked to convert the time derivative to a spatial derivative using an estimate of the sensor speed from shipboard GPS and the instrument pressure record. A typical sensor speed was 3 m/s, thus the Nyquist wavenumber is approximately 170 cpm. A typical response of the conductivity sensor was approximated as a single-pole filter with a cutoff frequency of 100 cpm. Spectra were computed for each 1 second data block and an estimate of the system noise was obtained by averaging spectra from the blocks with the lowest variance. This noise spectrum was subtracted from the gradient spectrum from each block prior to integrating over all wavenumbers to obtain an estimate of  $\chi_T^c$ .

The methodology suggested by Washburn et al. (1996) was used to correct the measured temperature variance dissipation rate for the effects of the sensor spatial response and the anti-aliasing filter and for the effect of salinity fluctuations on conductivity. We computed the T-S relationship ( $m = dS/dT$ ) as the slope of a linear fit to the 32 Hz T and S measurements over 3 second intervals. The kinetic energy dissipation rate ( $\epsilon$ ) was estimated based on the local overturning scale (note that although TOMASI is equipped with shear sensors, energetic vibrations of the towed body preclude their use at present). The overturning scale is computed from microconductivity variance computed over 1 second blocks ( $V_c$ ) and the local vertical conductivity gradient:

$$L = V_c \left( \frac{\partial C}{\partial z} \right)^{-1}$$

Assuming equivalence of the overturning scale ( $L$ ) to the Ozmidov scale ( $L_{Oz} = (\epsilon N^2)^{-1/2}$ ) and computing the buoyancy frequency allows estimation of  $\epsilon$ :

$$\epsilon \approx L^3 N^3$$

With valid estimates for  $m$  and  $\epsilon$ , the major uncertainty in the computed correction factor is the high-wavenumber correlation between T and S fluctuations. We therefore compute correction factors assuming both perfect correlation and zero correlation. The range of corrected  $\chi_T^2$  values then gives a measure of the uncertainty in the procedure. Data from an example tow is shown in Figure 4, showing the hydrographic structure, and Figure 5, showing the corrected  $\chi_T^2$  values, the correction factors, and the dissipation and T-S slope values used.

## IV. Results

$\chi_T^2$  values computed for each 1 second block were averaged for each tow in bins of 0.5 km by 1 dbar. These were combined with similar averages of the vertical temperature gradient  $dT/dz$  to provide estimates of the vertical eddy diffusivity ( $K_T$ ). Vertical sections of  $K_T$  are shown in Figures 6-8 for the three cruise periods. In these figures we show the eddy diffusivities estimated from corrected  $\chi_T^2$  using both assumptions as to the T-S correlation (perfect or zero correlation). The two eddy diffusivity estimates thus may be considered to represent the range of possible diffusivities. Eddy diffusivities computed assuming zero T-S correlation are lower than corresponding values computed assuming perfect correlation. The differences can be as large as a factor of 10, but the general patterns are similar. Near surface eddy diffusivities vary widely from survey to survey likely because of differences in wind mixing between the surveys. For example, strong winds were observed on 7/13 and 8/11-12. Near bottom diffusivities are generally higher during the 7/28-7/30 spring tide period than during the neap tide periods of 7/13-7/15 and 8/10-8/12. There also is evidence of enhanced mixing at a distance of 10-12 kilometers corresponding to the bottom depression coincident with a constriction in the estuary cross-section. This is also the area in which strong longitudinal gradients in temperature and salinity are observed in the surface and bottom layers and where a tongue of low oxygen water intrudes down estuary at mid-depth (Figure 4).

## V. References

Bergondo, D. L., D. R. Kester, H. E. Stoffel, and W. L. Woods, 2004. Time series observations during the low sub-surface oxygen events in Narragansett Bay during summer 2001. *Marine Chemistry*, (submitted).  
 Washburn, L., T. F. Duda, and D. C. Jacobs, 1996. Interpreting conductivity microstructure: Estimating the temperature variance dissipation rate. *J. Atmos. Oceanic Tech.*, 13: 1166-1188.

## VI. Acknowledgements

Funding for this work was provided by Rhode Island Sea Grant. Their support is gratefully acknowledged. The field work was carried out with the able assistance of Captain Tom Pickett, skipper of the URI vessel R/V Cap'n Bert. We thank Jim Fontaine for his efforts in the preparation of the equipment for the field efforts.